A&A 623, A84 (2018)
https://doi.org/10.1051/0004-6361/201834529

Astronomy & Astrophysics

The Arches cluster revisited

III. An addendum to the stellar census*

J. S. Clark[1], M. E. Lohr[1], L. R. Patrick[2,3], and F. Najarro[4]

[1] School of physical sciences, The Open University, Walton Hall, Milton Keynes MK7 6AA, UK
e-mail: s.clark@open.ac.uk
[2] Instituto de Astrofísica de Canarias, 38205 La Laguna, Tenerife, Spain
[3] Universidad de La Laguna, Dpto Astrofísica, 38206 La Laguna, Tenerife, Spain
[4] Departamento de Astrofísica, Centro de Astrobiología, (CSIC-INTA), Ctra. Torrejón a Ajalvir, km 4, 28850 Torrejón de Ardoz, Madrid, Spain

Received 29 October 2018 / Accepted 12 December 2018

ABSTRACT

The Arches is one of the youngest, densest and most massive clusters in the Galaxy. As such it provides a unique insight into the lifecycle of the most massive stars known and the formation and survival of such stellar aggregates in the extreme conditions of the Galactic Centre. In a previous study we presented an initial stellar census for the Arches and in this work we expand upon this, providing new and revised classifications for ∼30% of the 105 spectroscopically identified cluster members as well as distinguishing potential massive runaways. The results of this survey emphasise the homogeneity and co-evality of the Arches and confirm the absence of H-free Wolf-Rayets of WC sub-type and predicted luminosities. The increased depth of our complete dataset also provides significantly better constraints on the main sequence population; with the identification of O9.5 V stars for the first time we now spectroscopically sample stars with initial masses ranging from ∼16 $M_{\odot}$ to ≥120 $M_{\odot}$. Indeed, following from our expanded stellar census we might expect ≳50 stars within the Arches to have been born with masses ≳60 $M_{\odot}$, while all 105 spectroscopically confirmed cluster members are massive enough to leave relativistic remnants upon their demise. Moreover the well defined observational properties of the main sequence cohort will be critical to the construction of an extinction law appropriate for the Galactic Centre and consequently the quantitative analysis of the Arches population and subsequent determination of the cluster initial mass function.

Key words. stars: early-type – stars: Wolf-Rayet – stars: evolution – open clusters and associations: individual: Arches cluster – Galaxy: center

1. Introduction

Located within the central molecular zone (CMZ) of the Galaxy at a projected distance of ∼30 pc from SgrA*, the Arches is one of the most extreme young massive clusters in the Milky Way in terms of youth, integrated mass and stellar density. Independently discovered by Nagata et al. (1995) and Cotera et al. (1996), it has since become a lodestone for understanding the formation of very massive stars and starburst clusters in extreme conditions; the survival, structure and evolution of such aggregates in the gravitational potential of the Galactic centre; the form of the initial mass function and in particular the presence or otherwise of a high-mass cut-off; and the evolution and final end-points of the most massive stars nature permits to form in the local Universe.

Given this potential, much effort has been expended on constraining the form of the (initial) mass function via deep, high angular resolution photometric observations (e.g. Figer et al. 1999; Stolte et al. 2002; Kim et al. 2006; Espinoza et al. 2009; Clarkson et al. 2012; Habibi et al. 2013; Shin & Kim 2015; Hosek et al. 2018). However such efforts are compromised by significant uncertainties in the calibration of the mass/near-IR luminosity function, due to uncertainties over the form of the interstellar extinction law to apply which, in turn, yield errors of up to ∼0.6 dex in the bolometric luminosity of cluster members (Clark et al. 2018a; henceforth Paper I).

In parallel, multiple near-IR spectroscopic observations have been undertaken in order to better understand the constituent stars, construct a cluster HR diagram and hence infer fundamental properties such as cluster age and the masses of individual members (Figer et al. 2002; Najarro et al. 2004; Martins et al. 2008). Again prone to uncertainties regarding interstellar extinction, these studies have hinted at an extended formation history for cluster members, although Schneider et al. (2014) suggest this could instead result from binary interaction and rejuvenation.

Motivated by these efforts we undertook a multi-epoch spectroscopic study of the Arches in order to determine the properties of the binary population and, via the summation of multiple individual observations, obtain high signal-to-noise (S/N) spectra for the production of a stellar census, derivation of an extinction law and the quantitative determination of stellar and cluster parameters. Our initial census (Paper I) was based on three VLT/SINFONI observing runs in 2011, 2013 and 2017 that each remained substantially incomplete – a total of 16.4 h of observations were formally completed, with a further 10.1 h observations undertaken in non-optimal conditions. After acceptance of Paper I, a further 12.4 h and 1.8 h of observations were executed in optimal and non-optimal conditions between 2018

* Based on observations made at the European Southern Observatory, Paranal, Chile under programmes ESO 087.D-0317, 091.D-0187, 093.D-0306, 099.D-0345 and 0101.D-0141.

April-August. Additional multi-epoch VLT/KMOS observations were also made of a handful of brighter cluster members[1] as part of a wider survey of massive stars distributed thoughout the CMZ (Clark et al. 2018c); a number of stars in the vicinity of the Arches that had been flagged as potential runaways by Mauerhan et al. (2010) were also observed as part of this effort.

In this short supplemental paper we present the results from both observational programmes which, when combined with extant data, substantially improves on cluster completeness and yields much improved S/N spectra for a large number of cluster members, enabling more robust spectral classifications and quantitative analysis. The results of our radial velocity survey will be presented in a companion paper (Lohr et al., in prep.).

2. Data acquisition, reduction and analysis

Data acquisition and reduction for the VLT/SINFONI and VLT/KMOS observations closely followed the methodologies described in Clark et al. (2018a,b). The sole revision was in field placement for the SINFONI observations, which sampled a number of previously unobserved fields in the periphery of the cluster. These observations were undertaken between the nights of 2018 May 6 and August 23.

A total of 78 spectra were extracted from the VLT/SINFONI observations undertaken in 2018. Of these one is a previously unobserved cool star interloper (F36), which is not discussed further[2] and two are of spatially unresolvable blends of two cluster members, leading to spectra of 75 unique objects. Ten of these are the first observations of individual stars. After combination with extant data and the rebinning of 15 spectra to improve their S/N (at a cost of spectral resolution) the resultant dataset permitted analysis of a further eight previously unclassifiable objects (due to prior low S/N (3 stars) or potential blending (5 stars, see below)), with a revision of existing spectral type or luminosity class estimates possible for an additional 14 stars (Table 1). The remaining 44 spectra are consistent with current classifications (Paper I) but are of improved S/N. These data are still valuable since the greater S/N better constrains the shape of line profiles that are utilised in quantitative model-atmosphere analysis – an example being Brγ which is sensitive to wind properties.

We also took the opportunity to revisit objects that had previously been considered blends (Paper I). A number of stars are effectively merged with much brighter companions and hence are inaccessible[3]. F56+F95 and F57+72 are pairs of stars of comparble brightness that are fully blended and so we are only able to present composite spectra in order to demonstrate that the stars they derive from are not atypical when compared to the wider population. The blended F124 and F143 are likewise of comparable luminosity but are sufficiently faint to not justify extraction; as is F169, which is merged with a number of anonymous faint stars.

Inspection of the individual spectra of the previously unclassified stars F44 (close to F73), F73, F80 (close to F7), F142 (close to F53) and F170 (close to F32, F33 and F38) suggest that they are unlikely to be contaminated since the stellar features in their spectra differ in presence, strength and profile from their near neighbours. As a consequence we provide the first classifications for these objects (Sect. 3.1) but highlight their proximity to brighter neighbours in Table 1. No new observations were made of F166 (paper I); however its mid-O III-V star appearance is unexpected given its comparative faintness; hence we consider it likely that it is contaminated by its bright O hypergiant neighbour F27 and do not consider it further.

3. Data presentation, spectral classification and interpretation

As with data extraction and reduction, spectral classification followed the methodology outlined in Paper I. Spectra of the subset of cluster members for which categorisation – or revision of existing classifications – is now possible are presented in Figs. 1–3. Figure 4 presents a composite spectrum derived from multiple low S/N spectra of late-O main sequence candidates in comparison to template and synthetic classification spectra (Sect. 3.1), while in Fig. 5 we plot spectra of two unresolvable blends and a further four anomalous spectra. Finally, the spectra of potential runaways are shown in Fig. 6.

3.1. Cluster members

We present the first observations of F39, 41 and F48 in Fig. 1, finding them all to be new mid O supergiants (Table 1), as is the previously unclassified F44. F65 is likewise revised from luminosity class I-III to Ia. The spectral type of F23 is marginally earlier than prevously reported but importantly the strong narrow emission peak superimposed on the Brγ photospheric profile is found to be spurious (Fig. 1 and Table 1), as are similar features in F81 and F139 (Fig. 2 and Paper I). This is important as the shape and strength of this feature is an important diagnostic of stellar luminosity and wind properties; hence while the improved S/N of the new spectra of other cluster members may not affect their classification they will aid quantitative analysis.

Comparison of the previously unobserved stars F58 and F98 to classification templates reveals both to be mid-O giants (Fig. 1 and Table 1, although note the anomalously strong Brγ profile of F98) as are the previously unclassified F73 and F80 (Paper I). The much improved S/N of F131 allows a significant reclassification from >O8 V (Paper I) to O6.5 III (Fig. 2); surprising given its relative faintness in comparison to other giants. Despite proximity to both F10 and F17, inspection of their spectra suggests that they are unlikely to contribute to that of F131. Instead consideration of the IR colours of F131 and its spectroscopic twin F77 (Fig. 2) reveals the former to be redder, suggesting that it suffers anomalously high interstellar extinction[4]. Weaker emission in C IV 2.079 μm and the 2.11 μm blend implies a slightly later luminosity class for the newly observed F83 (O6-7 III-V; Fig. 2), bolstered by its similarity to F81. Finally, despite a low S/N which necessitated rebinning, the new spectrum of F94 is also consistent with such an identification (Fig. 3; noting the anomalously broad and strong Brγ profile).

Next we turn to the main sequence (MS) cohort (Figs. 2 and 3) where we provide the first classifications for eight stars and reclassifications for a further 11. Despite its comparatively low S/N even after rebinning, the presence of prominent C IV 2.089 μm emission and He II 2.189 μm absorption in the spectrum of F102 (Fig. 3) allows a refined classification of O5-6 V; the earliest spectral type sampled here. The strength of the He I

[1] Stars B1, F1, F6, F8, F9 and F16.

[2] For completeness F11, F36, F46, F51 and F99 are all interlopers.

[3] F31, F37, F66, F70, F76, F109, F122, F123, F140 and F167 are merged with F20, F7, F7, F1, F12, F7, F12, F28, F18, and F35, respectively.

[4] We highlight that F131 is located in the SW of the cluster; a region apparently subject to unexpectedly high reddening (cf. results for F2; Lohr et al. 2018).

Table 1. Expanded stellar population of the Arches cluster

ID	RA (h m s)	Dec (d m s)	m_{F127M} (mag)	m_{F139M} (mag)	m_{F153M} (mag)	m_{F205W} (mag)	#Observations (#Epochs)	Spectral classification	Notes
F23	17 45 51.211	−28 49 23.84	16.38	15.27	14.21	12.19	6(6)	O5.5-6 Ia	
F39	17 45 51.166	−28 49 36.70	16.98	15.84	14.76	12.65	1(1)	O5.5-6 Ia	
F41	17 45 50.429	−28 49 27.42	18.46	17.15	15.89	13.53	4(4)	O5 Ia	
F44	17 45 50.701	−28 49 25.59	17.19	16.05	14.93	12.88	7(5)	O5.5-6 Ia	Close to 73
F48	17 45 50.623	−28 49 26.96	17.69	16.53	15.42	13.28	6(6)	O5.5-6 Ia	
F56	17 45 50.591	−28 49 22.19	17.00	15.92	14.91	13.03	2(2)	*O5.5-6 III*	Merged with F95
F57	17 45 50.768	−28 49 20.31	16.91	–	–	13.04	2(2)	*O5.5-6 III*	Merged with F72
F58	17 45 49.968	−28 49 19.60	17.83	16.57	15.37	13.05	3(3)	O5.5-6 III	
F65	17 45 50.082	−28 49 21.53	17.58	16.42	15.32	13.16	5(5)	O5.5-6 Ia	
F72	17 45 50.784	−28 49 20.27	–	16.08	15.05	13.13	2(2)	*O5.5-6 III*	Merged with F57
F73	17 45 50.679	−28 49 25.58	17.78	16.59	15.48	13.35	11(9)	O6 III	Close to F44
F80	17 45 50.589	−28 49 19.46	17.40	16.29	15.32	13.47	28(14)	O6-6.5 III	Close to F7
F83	17 45 50.061	−28 49 20.67	18.00	16.81	15.69	13.53	4(4)	O6-7 III-V	
F89	17 45 50.955	−28 49 17.15	17.33	16.33	15.39	13.65	16(15)	O7-8 V	
F94	17 45 50.657	−28 49 28.03	18.74	17.50	16.33	14.14	4(4)	O6-8 III-V	
F95	17 45 50.578	−28 49 22.00	17.80	16.71	15.69	13.71	2(2)	*O5.5-6 III*	Merged with F56
F98	17 45 51.153	−28 49 37.06	18.08	16.93	15.87	13.75	1(1)	O6-6.5 III	
F101	17 45 50.914	−28 49 18.37	17.55	16.53	15.58	13.78	19(16)	O8 V	
F102	17 45 50.876	−28 49 28.80	18.24	17.07	15.93	13.78	6(6)	O5-6 V	
F118	17 45 50.453	−28 49 25.97	18.66	17.44	16.28	14.08	8(6)	O8-9.5 V	
F119	17 45 50.842	−28 49 22.75	18.18	17.09	16.06	14.06	11(10)	O8 V	
F121	17 45 50.204	−28 49 19.64	18.53	17.35	16.24	14.09	9(9)	O9.5 V	
F128	17 45 51.216	−28 49 36.53	18.51	17.37	16.28	14.18	1(1)	O9.5 V	
F130	17 45 50.605	−28 49 27.50	18.80	17.58	16.40	14.21	4(4)	O9.5 V	
F131	17 45 50.163	−28 49 27.46	19.11	17.80	16.55	14.23	9(6)	O6.5 III	Close to F10 & 17
F136	17 45 50.077	−28 49 27.84	19.59	18.18	16.83	14.30	13(10)	O6-7 V	
F139	17 45 51.207	−28 49 23.41	18.59	17.48	16.33	14.36	6(6)	O8 V	
F142	17 45 50.689	−28 49 24.93	18.63	17.50	16.43	14.41	2(2)	O8 V	Close to F53
F157	17 45 50.220	−28 49 24.18	19.11	17.89	16.71	14.55	14(14)	O8-9.5 V	
F159	17 45 50.882	−28 49 15.69	19.63	18.49	17.32	14.57	6(6)	O9.5 V	
F170	17 45 50.704	−28 49 20.96	18.74	17.67	16.63	14.74	19(10)	O8-9.5 V	Close to F32, 33 & 38
F173	17 45 50.204	−28 49 20.24	19.10	17.93	16.83	14.80	5(5)	O9.5 V	
F185	17 45 50.282	−28 49 27.56	19.65	18.40	17.18	14.95	10(7)	O9.5 V	
F186	17 45 50.001	−28 49 28.24	20.43	19.01	17.61	14.95	13(10)	O9.5 V	
F188	17 45 50.936	−28 49 21.80	19.02	17.93	16.91	14.97	3(3)	O9.5 V	
F189	17 45 50.595	−28 49 23.52	18.91	17.79	16.69	14.77	5(5)	O9.5 V	

Notes. We summarise the properties of stars with new or revised spectral classifications. Column 1 indicates the nomenclature for cluster members adopted by Figer et al. (2002), Cols. 2 and 3 the J2000 co-ordinates, Cols. 4–6 the HST WFC3 photometry from Paper I and Col. 7 F205W filter photometry from Figer et al. (2002). Column 8 presents the total number of VLT/SINFONI data-cubes available for individual objects, with the number in parentheses being the number of epochs on which these data were obtained. Column 9 provides a spectral classification while the final column provides additional notes on possible blending or contamination; individual cases are discussed in Sect. 2. F36 is found to be a cool interloper; as with F11, F46, F51 and F99 it is therefore excluded from the table. Finally the nominal classification of the unresolvable blends F56+F95 and F57+72 are given in italics.

2.112 μm and He II 2.189 μm temperature diagnostics suggest an O6 V classification for F136 although Brγ is anomalously strong and we see no evidence of (weak) C IV 2.089 μm emission; we adopt an initial (conservative) classification of O6-7 V. Of the remaining stars from Fig. 2, the presence of weak He II 2.189 μm absorption in F101 and F139 indicates that both are O8 V stars. The absence of this line and the strength of Brγ is consistent with an O9.5 V classification for F189, although the lack of O8.5 V and O9 V template spectra for comparison leaves open the possibility of a slightly earlier spectral type for this and other similarly classified stars. Intriguingly, the S/N of the F118 spectrum is sufficiently high to reveal an excellent coincidence between its He I 2.112 μm profile and that of the high $v\sin i$ O9.5 V template star HD 149757 (Hanson et al. 2005). One would also expect broadening in the He II 2.189 μm line in rapidly rotating stars and, given its comparative weakness in mid-late O stars, one might anticipate it being undetectable in relatively low S/N spectra, erroneously leading to the assignment of slightly later spectral types. Indeed rebinning the spectrum of F118 to improve the S/N suggests a possible detection of this feature; hence we assign an O8-9.5 V classification to this star.

As with F101 and F139 (Fig. 2), the strength of He II 2.189 μm and Brγ absorption, when combined with a lack of C IV 2.089 μm emission, suggests that F119 and F142 (Fig. 3) are both O8 V stars. A marginal detection of He II 2.189 μm in F157 results in an O8-O9.5 V classification. While this line appears absent in F170, the Brγ line appears unexpectedly weak for an

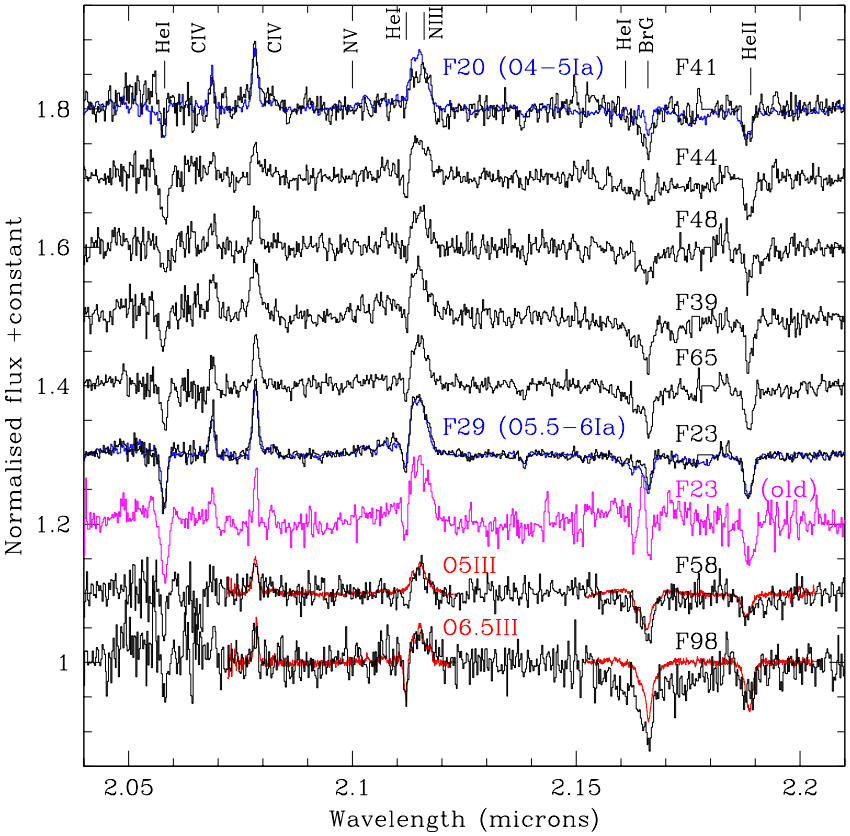

Fig. 1. *K*-band spectra of new or reclassified O4-6 giant and supergiant stars within the Arches. Spectra of supergiant cluster members F20 and F29 are shown for comparison (blue) as are the template spectra for O5 III (HD 15558) and O6.5 III (HD 190864) stars (red; Hanson et al. 2005). Finally the spectrum of F23 from Paper I is reproduced (magenta) in order to illustrate the increased S/N in the new data and also the removal of spurious emission in the Brγ profile of this particular star.

O9.5 V star (Fig. 3); hence we likewise adopt O8-O9.5 V for it. All the remaining stars in Fig. 3 lack He II 2.189 μm absorption and appear broadly consistent with O9.5 V classifications (subject to the *caveats* above), with the greater depth of the Brγ profile in F185 hinting at a still later spectral type. He I 2.112 μm absorption – present until spectral type B2-3 (e.g. Clark & Steele 2000) – appears absent in some sources (e.g. F159); we suspect this may be due to a combination of low S/N and an intrinsically broad, shallow line profile due to rapid rotation (cf. F118).

In order to verify these classifications we summed the spectra of our low-S/N O9.5 V candidates[5] to produce a single composite spectrum of higher S/N[6]. This is reproduced in Fig. 4 where an excellent correspondence is found with the O9.5 V template spectrum (Hanson et al. 2005). Foreshadowing future quantitative analysis and to further test our conclusions we also present illustrative synthetic spectra of O dwarfs generated with the non-LTE model-atmosphere code CMFGEN (Hillier & Miller 1998, 1999). We caution that we have not attempted to specifically fit the composite spectrum, adopting canonical effective temperatures for O8.5 V ($T_{\rm eff}$ ~ 32.5 kK) and O9.5 V stars ($T_{\rm eff}$ ~ 30.0 kK; following the calibration of Martins et al. 2005). A surface gravity of log g ~ 4.0 was employed and solar metallicity was assumed for the iron group elements, while we used a factor of two enhancement for α-elements with respect to iron (Najarro et al. 2009). Finally the resultant spectra were convolved with an assumed $v \sin i \sim 175$ km s^{-1} and degraded to the resolution of our observations.

The correspondence of both synthetic spectra with our composite spectrum is encouraging (Fig. 4). The He I 2.059 μm line is highly sensitive to the UV radiation field and while the He I 2.112 μm photospheric line appears a little strong, it is sensitive to both the turbulent velocity ($v_{\rm turb}$) and rotational broadening. However we find an excellent "fit" to the He I+Brγ photospheric blend in terms of both strength and line profile. Moreover our models predict emission in the Si IV ~2.427 μm blend, which is an excellent hot star diagnostic (cf. Clark et al. 2018b). This line is clearly in emission in our composite spectrum, with the unexpected breadth of the line likely due to incomplete correction of the significant telluric contamination that plagues this wavelength region. Given the consonance with both template and synthetic spectra we conclude that the individual component stars are indeed late-O dwarfs, with temperatures between 30–32 kK (footnote 5 and Table 1); assigning primacy to the template rather than synthetic spectra we classify these stars as O9.5 V.

Finally we turn to the anomalous spectra presented in Fig. 5. The blended spectra of F56+95 and F57+72 appear to resemble mid-O giants; as a consequence it appears unlikely that any of the constituent stars differ greatly from the wider population. As to F92 and F93, the presence of emission in the He I/N III/O III/C III 2.11 μm blend and C IV 2.079 μm line, when combined with He I 2.059 μm absorption (and for F92 also He I 2.112 μm) is likewise consistent with a mid-O classification (Table 1). However the absence of pronounced Brγ and He II 2.189 μm photospheric lines is unexpected. Some trace of the latter may be evident in both spectra; the same may be true for Brγ in F93, while weak, broad emission may be present in F92.

[5] F121, F128, F130, F159, F173, F186 and F188.

[6] Excluding the significant overheads associated with telescope preset, instrumental set-up, target acquisition and telluric observations for the multiple observations used to construct the composite spectrum, but including sky observations and overheads associated with read-out, this amounts to a total of ~4.6 h of observations, of which time-on-target is 60% of this total.

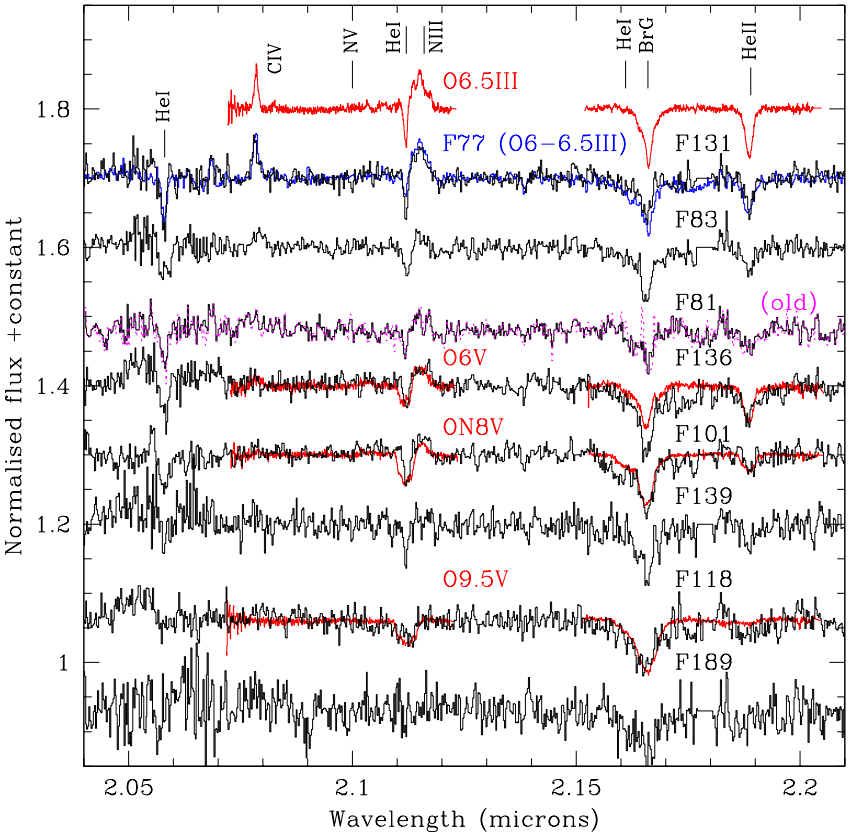

Fig. 2. *K*-band spectra of new or reclassified O6-O9.5 main sequence and giant stars within the Arches. A spectrum of the O6-6.5 III cluster member F77 is shown for comparison (blue) as are the template spectra for O6.5 III (HD 190864), O6 V (HD 5689), ON8 V (HD 13268) and O9.5 V (HD 149757) stars (red; Hanson et al. 2005). Finally the spectrum of F81 from Paper I is reproduced (magenta) in order to illustrate the removal of spurious emission in the Brγ profile.

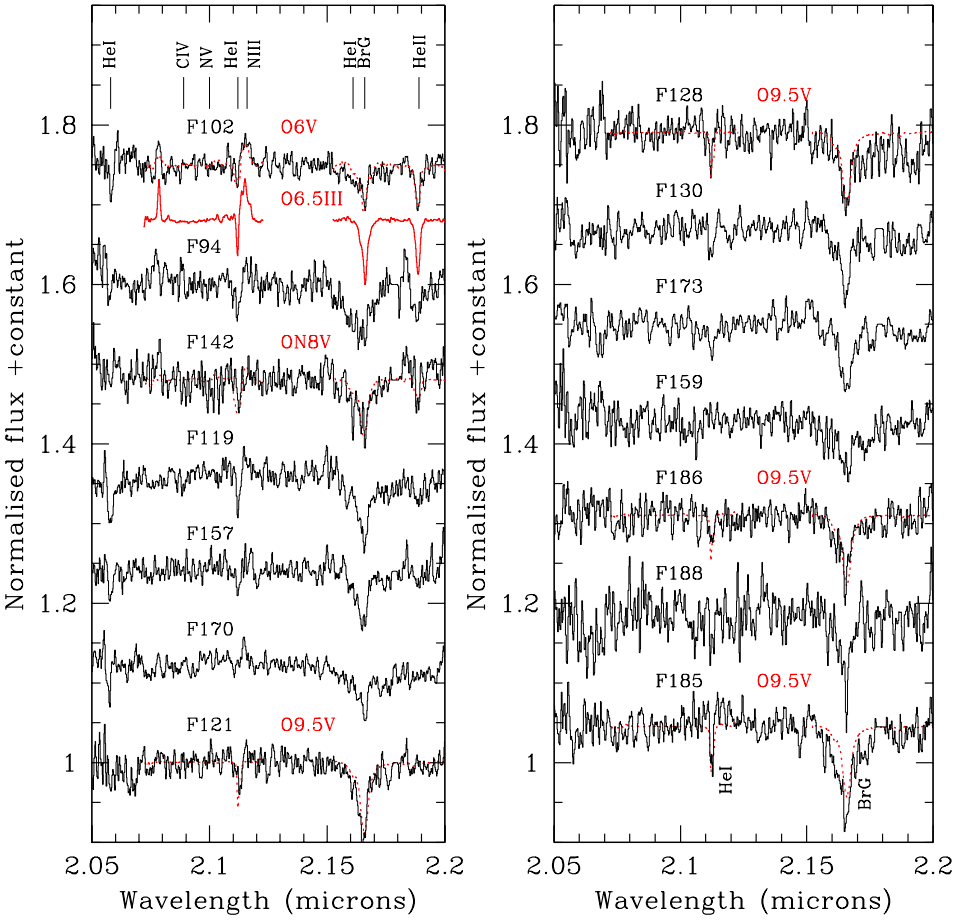

Fig. 3. *K*-band spectra of additional giant and main sequence cluster members; these have been rebinned to improve the S/N. Comparison spectra for O6 V (HD 5689), O6.5 III (HD 190864), ON8 V (HD 13268) and O9.5 V (HD 37468) are overplotted in red and from Hanson et al. (2005).

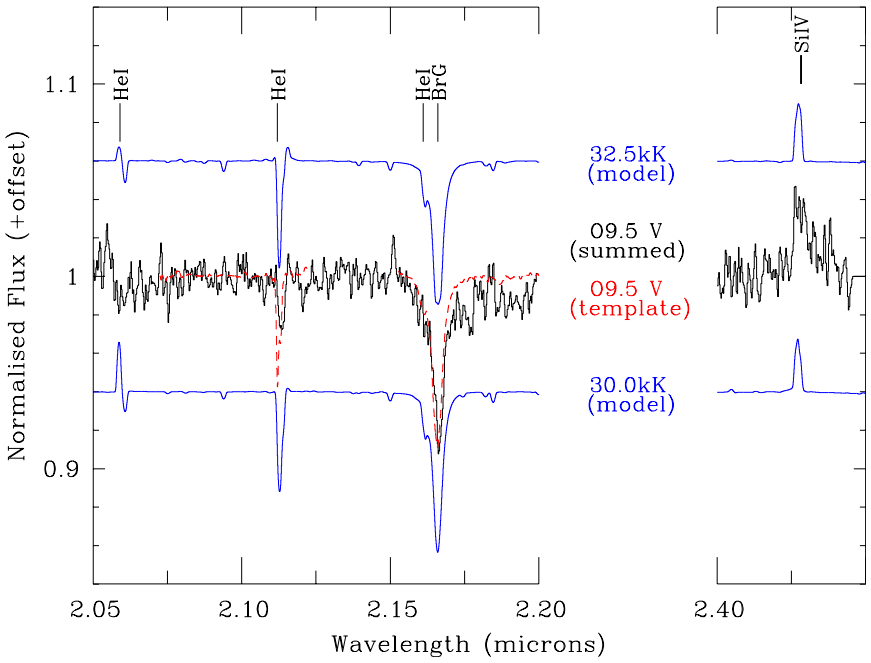

Fig. 4. *K*-band spectrum derived from the combination of individual spectra of candidate O9.5 V stars (black) plotted against template O9.5 V spectrum (HD 37468) and synthetic spectra for 32.5 kK and 30.0 kK O dwarfs (blue; Sect. 3.1). The region of the spectrum between 2.2 μm and 2.4 μm is both predicted and found to be featureless.

Motivated by these findings we examined the longer wavelength portion of both spectra. CO bandhead emission is absent for both sources but Si IV ~2.427 μm is present, confirming both are early-type stars. Additionally weak N III 2.247 μm and 2.251 μm emission is present in F92; unfortunately the S/N of F93 is too poor for conclusions to be drawn. The combination of Si IV and N III emission is seen in mid O giants such as F77, corroborating the classifications derived from shorter wavelength diagnostics. We speculate that excess emission from unexpectedly strong stellar winds may result in the infilling of the Brγ and He II 2.189 μm photospheric lines for both stars; the lack of CO bandhead emission arguing against a contribution from a cool circumstellar disc (such as found for a subset of low luminosity cluster members; Stolte et al. 2010, 2015).

The spectra of F150 and F151 appear to represent even more extreme examples of this phenomena – emission in Brγ and the 2.11 μm blend (with He I 2.112 μm absorption) is present in the former while the latter is entirely featureless. Again CO bandhead emission is absent from these stars while the low S/N of the spectra in this region preclude conclusive identification of Si IV emission. Noting that both stars are magnitudes fainter than the dust-enshrouded WCL stars found within the Quintuplet (Paper I, Clark et al. 2018b) we are unable to offer an evolutionary classification for these objects, but simply assume that the spectra are dominated by emission from circumstellar material.

3.2. Runaways

Mauerhan et al. (2010) discuss three stars identified by the Paα survey of Dong et al. (2011) as potential runaways – [DCW2011] P19, P22 and P96 (=#11 and #12 and G0.10+0.02, respectively, in the former work) – which are all located at a projected distance of 1–2 pc from the Arches. To these we may add a fourth, [DCW2011] P97, at a slightly larger distance of 4–5 pc (Dong et al. 2015).

Comparison of our spectrum of [DCW2011] P19 to that of the Quintuplet cluster member LHO158 (Fig. 6) shows a striking resemblance, slightly refining the spectral classification to that of an anomalously broad-lined WN9h star. Such stars likely have lower temperatures and mass-loss rates than the least extreme WN7-9ha stars within the Arches (which at 2–3 Myr is younger than the 3–3.6 Myr old Quintuplet; Paper I, Clark et al. 2018b); hence we consider its physical association with the cluster unproven at this time.

In contrast Mauerhan et al. (2010) classify [DCW2011] P22 as WN8-9h; comparison of their spectrum to the WNLh cohort in the Arches shows a close correspondence to the least extreme example, F16. The only previous spectra of [DCW2011] P96 were of low resolution and S/N (Cotera et al. 1999); our new observation shows it to be a doppleganger of the WN7-8h star F4 (Fig. 6) and we adopt this as a classification. Finally Dong et al. (2015) suggest O4-6 Ia$^+$ for [DCW2011] P97; on the basis of its marked similarity to F15 we slightly revise this to O6-7 Ia$^+$.

Considering photometric observations and the *H*- and *K*-band magnitudes of [DCW2011] P22 and P97 deviate from their Arches comparators by only 0.1mag in the *K*-band (Dong et al. 2011). [DCW2011] P96 is significantly fainter than F4 but is also redder, suggesting differential extinction may cause this discrepancy; in any event it lies within the envelope of magnitudes exhibited by the population of WNLh stars within the Arches.

Assuming a runaway velocity of ~10 km^{-1} it would take only ~98 000 yr (~244 000 yr) to travel a projected distance of 2 pc (5 pc) from the Arches, significantly less than the age of the cluster (~2–3 Myr; Paper I). Given this and the close equivalence of both spectroscopic and photometric properties of [DCW2011] P22, P67 and P97 to Arches members, we consider it likely that they are indeed runaways from the cluster; either as a result of dynamical interactions (e.g. Poveda et al. 1967) or tidal stripping/disruption (e.g. Habibi et al. 2014; Park et al. 2018). Moreover it is unlikely that these stars comprise the complete runaway population; other stars of comparable spectral type are located at larger distances throughout the CMZ, while the O supergiants (and less evolved stars) found within the Arches support weaker winds and hence will not have been detected by the Paα survey of Dong et al. (2011).

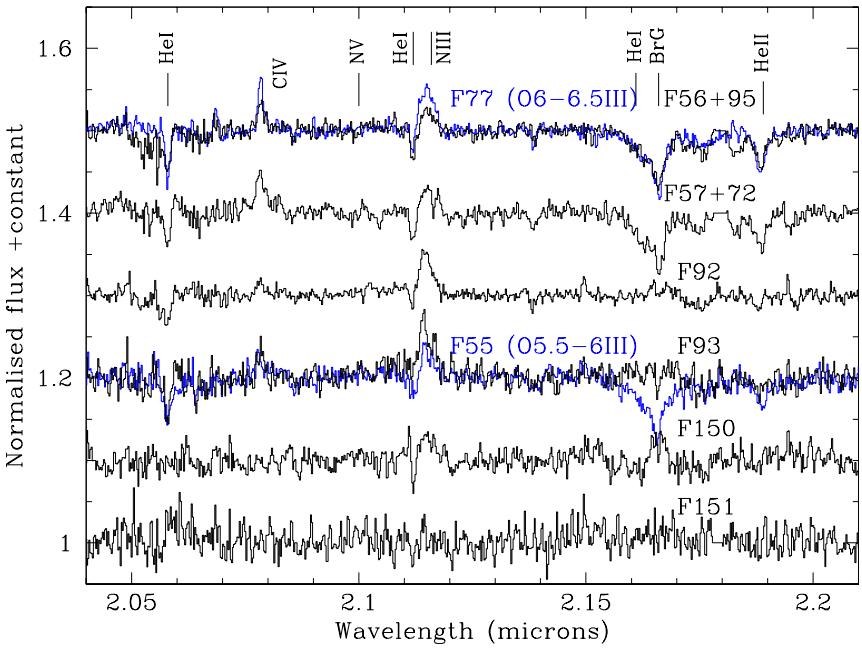

Fig. 5. *K*-band spectra of the blends of F56+F95 and F57+72 along with the anomalous souces F92, F93, F150 and F151 (see Sect. 3.1). Spectra of the cluster members F55 and F77 are overplotted in blue for comparison.

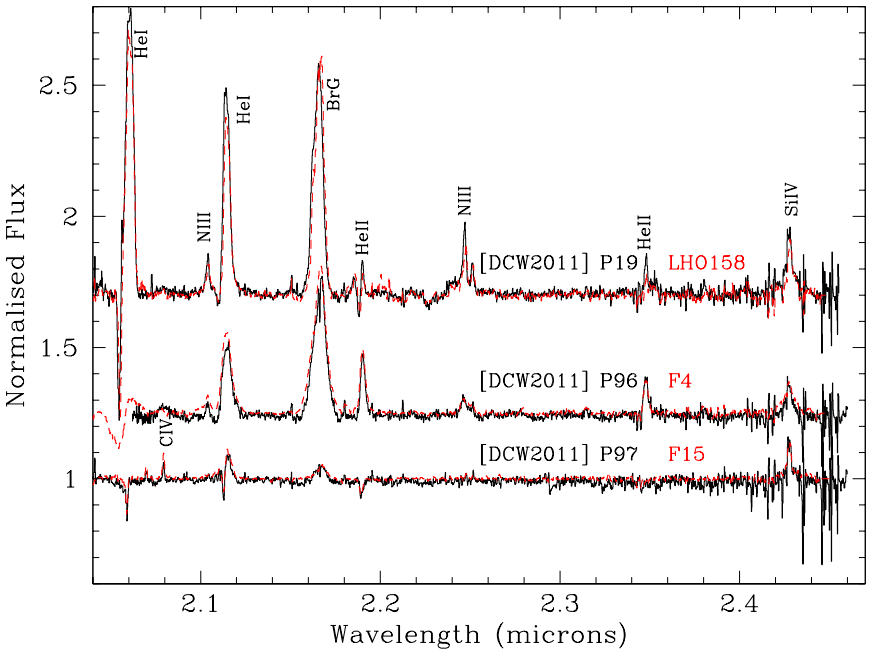

Fig. 6. *K*-band spectra of candidate runaways (black) compared to members of the Arches and Quintuplet (red; Clark et al. 2018a,b). [DCW2011] P96 and P97 show a close resemblance to WN7-8h and O6-7 Ia$^+$ stars within the Arches, while [DCW2011] P19 corresponds to the sole broad-lined WN9h star within the older Quintuplet.

4. Discussion and concluding remarks

4.1. Observational completeness

At this juncture it is worth considering the completeness of the current sample. We are now able to provide spectral classifications for a total of 105 cluster members. This includes the first classifications for 18 stars and the reclassification of a further 14 objects, but excludes two unclassifiable stars (F150 and F151), the unresolvable blends F56+F95 and F57+72 and the three putative runaways (Sect. 3.2). Stars F1-F51, B1 and B4 have all been observed multiple times, and have either been identified as cluster members (47 objects; Paper I and Table 1), rejected as non-members (F11, 36, 46 and 51) or were too close to other, brighter stars to extract a useful spectrum (F31 and 37). With the exception of F41 and F50, these correspond to stars with $m_{\rm F205W} \sim 10.4-12.9$ (Figer et al. 2002). Excluding blends and interlopers (seven objects; Sect. 2), in the range F52–F100 ($m_{\rm F205W} \sim 12.9-13.8$) 28 stars have spectra of sufficient quality to allow classification as bona fide cluster members. Thus, of the 102 brightest stars potentially associated with the Arches we identify 75 as constituents, with only 13 objects remaining to be observed[7].

Of the remaining 96 stars identified by Figer et al. (2002; F101-196 ($m_{\rm F205W} \sim 13.8-15.0$)) observations of sufficient S/N for classification have been made for 29 objects (Paper I and Table 1). Spectra of five stars were of insufficient S/N to permit this[8], while a further four objects were judged too faint to make extraction worthwhile[9]. Of the remainder, seven stars are

[7] F52, F59, F61, F67, F71, F75, F78, F79, F86, F88, F91, F97 and F100.
[8] F166, F168, F174, F176 and F184.
[9] F158, F163, F182 and 187.

inaccessible due to blending (Sect. 2) leaving 48 that are still to be observed[10]; however it appears likely that many of these will likewise prove too faint or contaminated to justify observation. Hence we consider that the current census is approaching the limits of what is achievable with 8m-class telescopes and modern instrumentation under reasonable time constraints and, for the most evolved stars, is indeed essentially complete.

Finally, for completeness we note that the census does not sample the additional population of *L*-band excess stars which, via the presence of CO-bandhead emission, appear to support cool, dusty circumstellar discs (Stolte et al. 2010, 2015).

4.2. Properties of the Arches stellar population

We may summarise the current stellar census of the Arches as follows (Paper I and Table 1):

- 13 Wolf Rayets, comprising two WN7-8ha and eleven WN8-9ha subtypes.
- Eight O hypergiants with spectral types ranging from O4-5 to O7-8.
- 30 O supergiants spanning a restricted range of spectral types (O4 to O6).
- Five lower luminosity O4-O6 I-III (super-)giants.
- Ten O5-6.5 III giants.
- Seven stars with spectral types ranging from O5-6 to O7-8 and of uncertain (III-V) luminosity class.
- 32 main sequence stars with spectral types spanning O5-6 V to O9.5 V.

Following the discussion of completeness in Sect. 4.1, for any reasonable (initial) mass function (cf. Sect. 1) we are likely to be somewhat incomplete for the main sequence component of the Arches. Conversely, given the magnitudes of the currently identified Wolf-Rayet and O hypergiants, we are likely to be essentially complete for both cohorts, and largely complete for the O supergiants; only three stars that are brighter than the current faintest O supergiant (F65) remain to be observed.

The expanded census again emphasises the remarkable homogeneity of the cluster membership (cf. Paper I). Unlike the older Quintuplet (∼3−3.6 Myr) and Westerlund 1 (∼5 Myr) we find no examples of H-free WC stars within the Arches (∼2−3 Myr; Clark et al. 2005, 2018b; Crowther et al. 2006). We emphasise that the faintest WC stars within the Quintuplet – which derive from stars with initial masses comparable to those observed here – have $m_{\rm F205W} \sim 11.7$ (Clark et al. 2018b); a magnitude at which we are observationally complete (Sect. 4.1). Likewise the distribution of WN spectral sub-types within the Arches is much narrower than seen in either of these clusters (Clark et al. 2018b; Crowther et al. 2006). Similarly, we see no evidence for the earlier – and highly luminous – WN5-7ha and O2-3 Ia stars found within younger clusters such as NGC 3603 (∼1−2 Myr; Melena et al. 2008; Roman-Lopes et al. 2016) and R136 ($\sim 1.5^{+0.3}_{-0.7}$ Myr; Crowther et al. 2016). Finally, while we cannot exclude the possibility of massive blue stragglers within the cluster, we find no evidence to mandate their presence; this contrasts with the presence of demonstrably younger stellar members in both the Quintuplet and Wd1 (Clark et al. 2018b, 2019).

The absence of the very earliest O spectral sub-types extends to the less-evolved stellar cohorts of the Arches. Our much expanded MS census suggests an absence of O2-4 stars, with the earliest stars present classified as O5-6 III-V or O5-6 V[11]. Thus a MS turn-off around O4 V is still favoured; implying a surprisingly conservative turn-off mass of ∼30−40 $M_\odot$ (following the dynamically determined spectral type/mass relation presented in Paper I). At the fainter end we are able to (re-)classify a large number of stars with previously low S/N spectra from ≥O8 V to ∼O9.5 V (noting that, in the absence of observational templates, our synthetic spectra suggest O8.5 V stars may be similar in appearance; Fig. 4). Therefore it would seem likely that the remaining stars with this preliminary classification (Paper I) are similarly only slightly later in spectral type. Again following Paper I, we estimate a mass of ∼16 $M_\odot$ (∼22 $M_\odot$) for the O9.5 V (O8.5 V) stars.

4.3. Synopsis and future directions

The inclusion of data from the 2018 observing season has significantly expanded upon the stellar census presented in Paper I, allowing the first classifications of 18 stars and re-classification of a further 14; ∼30% of a total of 105 classified cluster members (which does not include a further four deeply blended objects nor two stars with anomalous, unclassifiable spectra: Sect. 3.1). Our results buttress conclusions from Paper I; the Arches appears highly homogeneous and hence likely co-eval, with no evidence for H-free Wolf-Rayets nor the products of binary interaction, although we may not exclude the presence of the latter at this time. Comparison to the cluster population suggests that three isolated, very massive stars ≤5 pc (projected) from the Arches are potential runaways either stripped from the cluster by tidal forces or ejected via dynamical interactions, with the nature of a fourth currently uncertain.

The enlarged and better-constrained MS population is arguably the most valuable product of this study. We find an apparent MS turn-off around O4-5 V, and classify a large number of O9.5 V stars for the first time. The initial masses of spectroscopically classified stars within the Arches therefore ranges from ∼16 $M_\odot$ for the O9.5 V stars through to ≥120 $M_\odot$ for the WN8-9ha primary of F2 (Lohr et al. 2018). Filling in the gaps and masses in the ∼30−40 $M_\odot$ range are suggested for the O5-6 V cohort that delineates the MS turn-off (Sect. 4.2). A current mass of 60 ± 8 $M_\odot$ was determined for the O5-6 Ia$^+$ secondary of F2 (Lohr et al. 2018); however simulations by Groh et al. (2014) suggest that non-rotating stars of 60 $M_\odot$ do not pass through such a phase, implying that mid-O hypergiants must instead evolve from stars of higher initial mass; a result supported by the independent calculations of Martins & Palacios (2017). Groh et al. (2014) further demonstrate that in the 1.7–3 Myr window 60 $M_\odot$ stars will appear as, progressively, O4 Ia to O7 Ia supergiants; consistent with both the estimated age of the Arches and the distribution of supergiant spectral types (Paper I and Table 1).

If correct, following from the population breakdown in Sect. 4.2 the Arches would host at least 51 stars with initial masses ≳60 $M_\odot$ (WRs and O super-/hypergiants, but excluding the putative runaways from this count) with a subset likely over twice this value. In contrast the Quintuplet hosts a minimum of 38 stars with initial masses ≳60 $M_\odot$ (Clark et al. 2018b); however this is likely to be an underestimate since the current survey is significantly incomplete and the count does not include potential binary-interaction products nor the large population of H-free WC stars which do not conform to the predictions of Groh et al. (2014).

[10] F103-109, F111, F113, F116, F120, F125-127, F129, F132-134, F137, F138, F141, F144-149, F152, F154, F156, F160-162, F164, F165, F171, F175, F178-181, F183, and F190-196.

[11] F82 and F87, F90, F92, F102 and F115, respectively.

The consequences of such a stellar cohort are striking. Within the next ~10 Myr, we might expect all 105 spectroscopically classified members of the Arches to undergo core-collapse, leaving relativistic remnants behind (Groh et al. 2013). The incomplete nature of our current MS census – and indeed our insensitivity to stars $<15\,M_{\odot}$ – coupled with the possibility of a substantial population of massive binaries (Lohr et al., in prep.) suggests that this may be a significant underestimate of the true number. Evidently clusters such as the Arches and Quintuplet are important engines for the injection of neutron stars and black holes into the Galactic CMZ.

Moving forward, the increased S/N of many of the Arches spectra will greatly aid in quantitative model-atmosphere analysis even where no spectral re-classification was warranted. Critically, the well defined observational properties of our expanded MS cohort will permit the simultaneous determination of an extinction law appropriate for the galactic centre; these efforts will be published in a future work. The numerous dynamical mass determinations available for O5-O9.5 V stars (Paper I) will inform calibration of the mass/luminosity function for the Arches and hence the formulation of the cluster initial mass function. Likewise the physical parameters of the cluster members determined via modelling will allow the construction of an HR diagram; allowing current evolutionary predictions for very massive stars to be tested and bulk cluster properties such as age and radiative and mechanical feedback to be constrained.

Acknowledgements. Based on observations collected at the European Organisation for Astronomical Research in the Southern Hemisphere under ESO programmes 087.D-0317, 091.D-0187, 093.D-0306, 099.D-0345 and 0101.D-0141. This research was supported by the Science and Technology Facilities Council. FN acknowledges financial support through Spanish grants ESP2015-65597-C4-1-R and ESP2017-86582-C4-1-R (MINECO/FEDER).

References

Clark, J. S., & Steele, I. A. 2000, A&AS, 141, 65
Clark, J. S., Negueruela, I., Crowther, P. A., & Goodwin, S. P. 2005, A&A, 434, 949
Clark, J. S., Lohr, M. E., Najarro, F., Dong, H., & Martins, F. 2018a, A&A, 617, A66
Clark, J. S., Lohr, M. E., Patrick, L. R., et al. 2018b, A&A, 618, A2
Clark, J. S., Lohr, M. E., Najarro, F., et al. 2018c, The Messenger, 173, 22
Clark, J. S., Najarro, F., Negueruela, I., et al. 2019, A&A, in press, DOI 10.1051/0004-6361/201834245
Clarkson, W. I., Ghez, A. M., Morris, M. R., et al. 2012, ApJ, 751, 132
Cotera, A. S., Erickson, E. F., Colgan, S. W. J., et al. 1996, ApJ, 461, 750
Cotera, A. S., Simpson, J. P., Erickson, E. F., et al. 1999, ApJ, 510, 747
Crowther, P. A., Hadfield, L. J., Clark, J. S., Negueruela, I., & Vacca, W. D. 2006, MNRAS, 372, 1407
Crowther, P. A., Caballero-Nieves, S. M., Bostroem, K. A., et al. 2016, MNRAS, 458, 624
de Mink, S. E., Sana, H., Langer, N., Izzard, R. G., & Schneider, F. R. N. 2014, ApJ, 782, 7
Dong, H., Wang, Q. D., Cotera, A., et al. 2011, MNRAS, 417, 114
Dong, H., Mauerhan, J., Morris, M., Wang, Q. D., & Cotera, A. 2015, MNRAS, 446, 842
Espinoza, P., Selman, F. J., & Melnick, J. 2009, A&A, 501, 563
Figer, D. F., Kim, S. S., Morris, M., et al. 1999, ApJ, 525, 750
Figer, D. F., Najarro, F., Gilmore, D., et al. 2002, ApJ, 581, 258
Groh, J. H., Meynet, G., Georgy, C., & Ekström, S. 2013, A&A, 558, A131
Groh, J. H., Meynet, G., Ekström, S., & Georgy, C. 2014, A&A, 564, A30
Habibi, M., Stolte, A., Brandner, W., Hußman, B., & Motohara, K. 2013, A&A, 556, A26
Habibi, M., Stolte, A., & Harfst, S. 2014, A&A, 566, A6
Hanson, M. M., Kudritzki, R.-P., Kenworthy, M. A., Puls, J., & Tokunaga, A. T. 2005, ApJS, 161, 154
Hillier, D. J., & Miller, D. L. 1998, ApJ, 496, 407
Hillier, D. J., & Miller, D. L. 1999, ApJ, 519, 354
Hosek, M. W., Lu, J. R., Anderson, J., et al. 2018, ApJ, 870, 44
Kim, S. S., Figer, D. F., Kudritzki, R. P., & Najarro, F. 2006, ApJ, 653, L113
Lohr, M. E., Clark, J. S., Najarro, F., et al. 2018, A&A, 617, A66
Martins, F., & Palacios, A. 2017, A&A, 598, A56
Martins, F., Schaerer, D., & Hillier, D. J. 2005, A&A, 436, 1049
Martins, F., Hillier, D. J., Paumard, T., et al. 2008, A&A, 478, 219
Mauerhan, J. C., Cotera, A., Dong, H., et al. 2010, ApJ, 725, 188
Melena, N. W., Massey, P., Morrell, N. I., & Zangari, A. M. 2008, AJ, 135, 878
Nagata, T., Woodward, C. E., Shure, M., & Kobayashi, N. 1995, AJ, 109, 1676
Najarro, F., Figer, D. F., Hillier, D. J., & Kudritzki, R. P. 2004, ApJ, 611, L105
Najarro, F., Figer, D. F., Hillier, D. J., Geballe, T. R., & Kudritzki, R. P. 2009, ApJ, 691, 1816
Park, S.-M., Goodwin, S. P., & Kim, S. S. 2018, MNRAS, 478, 183
Poveda, A., Ruis, J., & Allen, C. 1967, BOTT, 4, 86
Roman-Lopes, A., Franco, G. A. P., & Sanmartim, D. 2016, ApJ, 823, 96
Schneider, F. R. N., Izzard, R. G., de Mink, S. E., et al. 2014, ApJ, 780, 117
Shin, J., & Kim, S. S. 2015, MNRAS, 477, 366
Stolte, A., Grebel, E. K., Brandner, W., & Figer, D. F. 2002, A&A, 394, 459
Stolte, A., Morris, M. R., Ghez, A. M., et al. 2010, ApJ, 718, 810
Stolte, A., Hußmann, B., Olczak, C., et al. 2015, A&A, 578, A4